

## SPIN-ORBIT ANGLE DISTRIBUTION AND THE ORIGIN OF (MIS)ALIGNED HOT JUPITERS

A. Crida<sup>1</sup> and K. Batygin<sup>2</sup>

**Abstract.** The angle between the orbital plane and the stellar equator (called the spin-orbit angle) has been measured for about 60 hot Jupiters, half of them showing significant misalignment. This challenges scenarios of the formation of hot Jupiters. Recently, it has been proposed that misalignment could be a consequence of the torquing of the proto-planetary disk by a transient binary companion of the host star.

Here, we analyse the geometry of the problem, and compare the probability density function (PDF) of the projected spin-orbit angle expected in various mechanisms, with the observed one. Scattering models and the Kozai cycle with tidal friction models can not be solely responsible for the production of all hot Jupiters. Conversely, the presently observed distribution of the spin-orbit angles is compatible with most hot Jupiters having been transported by smooth migration inside a proto-planetary disk, itself possibly torqued by a companion.

Keywords: Planets and satellites: formation, Planets and satellites: dynamical evolution and stability, Planet-disk interactions, Methods: statistical

### 1 Introduction

As stars spin, part of their surface moves towards us, while on the other side, the surface moves away from the observer. As a consequence, half of a star is slightly blue-shifted and the other half red-shifted, which results in a broadening of the spectral lines. When an exoplanet transits in front of its star, it blocks successively the light coming from regions with a different redshift. This results in a signal in the radial velocity measurement of the star, called the Rossiter - Mac Laughlin effect (Mac Laughlin 1924). Using this, one can infer the angle between the stellar spin axis and the trajectory of the planet, projected on the plane of the sky (e.g., Winn et al. 2007; Triaud et al. 2010). This angle is called the “spin-orbit angle”, generally noted  $\beta$  or  $\lambda$ .

The 61 measurements known to date are binned in the histogram shown on Figure 1. They all concern hot Jupiters, giant planets with short periods, for which the measure is easier. While 34 are measured to be smaller than  $20^\circ$ , that is compatible with perfect alignment of the orbital plane and the equatorial plane of the star, half of them show misalignment, and even retrograde orbits ( $\beta > 90^\circ$ ). This questions the origin of these planets. While most researchers consider that in situ formation of hot giant planets is very unlikely, two kinds of mechanisms have been invoked to move a giant planet close to its parent star: (i) early, smooth migration in the plane of the gaseous proto-planetary disk (Lin & Papaloizou 1986; Crida & Morbidelli 2007), (ii) late, more violent orbital change due to planet-planet scattering, Kozai resonance with a companion, or tidal interaction with the central star and combinations of these processes (e.g. Rasio & Ford 1996; Ford & Rasio 2008; Fabrycky & Tremaine 2007; Naoz et al. 2011). In case (ii), a change of the orbital plane is likely, causing spin-orbit misalignment. In case (i), the orbital plane stays in the proto-planetary disk plane, supposedly equal to the stellar equatorial plane; however, (Batygin 2012) has shown that the proto-planetary disk could precess around the axis of a transient stellar companion, so that smooth migration is not incompatible with spin-orbit misalignment. In Crida & Batygin (2014), we analyse the distribution of the spin-axis angle, with a careful analysis of projection effects, and compare it with the distribution expected for various mechanisms. These results are briefly presented here, where section 2 explains how to link the real spin-orbit angle to the projected one on the plane of the sky, and section 3 compares observations with a few mechanisms available in the literature.

---

<sup>1</sup> Laboratoire Lagrange, UMR 7293 ; Universit  Nice Sophia-antipolis / CNRS / Observatoire de la C te d’Azur ; Boulevard de l’Observatoire, CS 34229, 06300 Nice, FRANCE. [crida@oca.eu](mailto:crida@oca.eu)

<sup>2</sup> Institute for Theory and Computation, Harvard-Smithsonian Center for Astrophysics, 60 Garden St., Cambridge, MA 02138, USA.

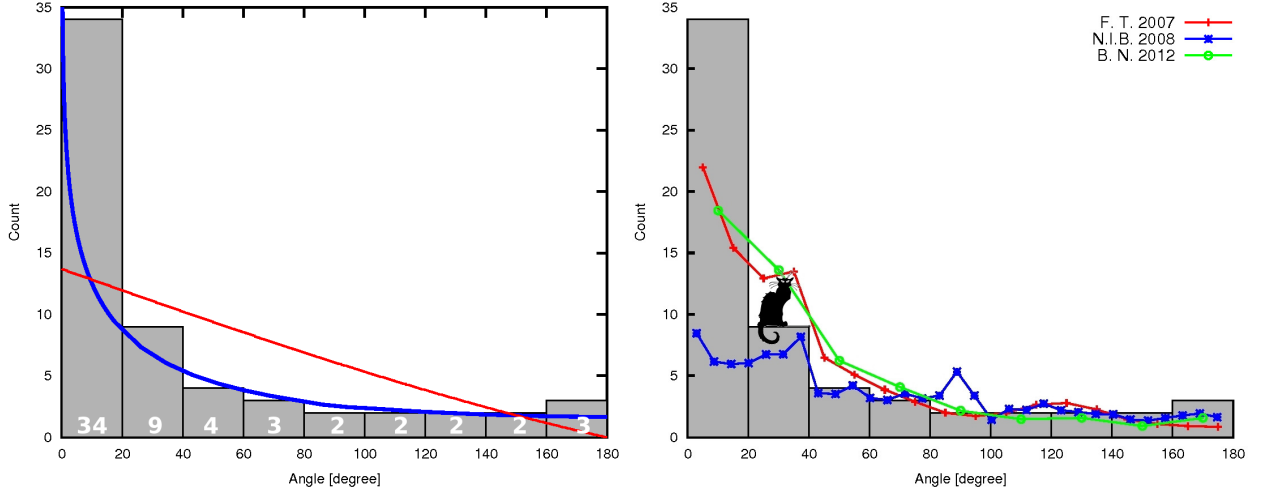


**Fig. 1.** Grey-shaded histogram: observed projected spin-orbit angle  $\beta$  (taken as  $|\beta|$  or  $|\lambda|$  in the data from [exoplanets.org](http://exoplanets.org)). **Left**: red thin line: distribution of  $\Psi$ , given by Eq. (3.1); blue thick line: corresponding PDF of  $\beta$ . **Right**: red line with + symbols labelled F.T. 2007: distribution of  $\beta$  expected in the Fabrycky & Tremaine (2007) mechanism of Kozai cycles with tidal friction (their Fig. 10b providing  $\Psi$  in bins of  $10^\circ$ ); blue line with stars labelled N.I.B.2008: distribution found by Nagasawa et al. (2008) in their model of planet-planet scattering, tidal circularisation, and Kozai mechanism (their fig. 11c); green line with circles labelled B.N.2012: example of distribution found by Beaugé & Nesvorný (2012) in their model of multi-planet scattering (their fig. 16). All the distributions of  $\beta$  have been normalised to have 18 cases with  $\beta > 40^\circ$ , for an easier comparison.

## 2 The 3D geometry of the spin-orbit angle and projection effects

The true misalignment angle is actually the angle between two vectors in 3D space:  $\vec{L}_p$ , the orbital angular momentum of the planet, and  $\vec{L}_s$ , the angular momentum of the spin of the star. As such, it can only lie between 0 and 180 degrees (there are no negative angles in 3D). This real, 3D angle is denoted below as  $\Psi$ . For a fixed  $\Psi$ , which  $\beta$  will be observed? What is the probability density function (PDF) of  $\beta$ ?

On Figure 2, the yellow sphere is the unit sphere, centred on the star O, and the vertical axis is  $\vec{L}_p$ . The stellar spin axis  $\vec{L}_s$  points towards S, whose colatitude is  $\Psi$  by definition, and longitude (azimuth)  $\phi_s$ , unknown. The top left panel is the circle gathering all the points of colatitude  $\Psi$ , so that  $A'A = A'S = A'R = \sin \Psi$  and  $A'S' = \sin \Psi |\sin \phi_s|$ .

In the projected plane (shown in bottom left of Fig. 2), the angle between the north pole of the orbit and the spin of the star appears to be  $\beta = \widehat{A'OS'}$ . One can see that  $\tan \beta = A'S'/OA'$ , where  $OA' = \cos \Psi$  is negative when  $\Psi > \pi/2$ . Finally,

$$\beta = \arctan(|\sin \phi_s| \tan \Psi) \equiv G(\phi_s) \quad (2.1)$$

As the distribution of  $\phi_s$  is uniform in the interval  $[0; 2\pi[$ , and  $|\sin(x)| = |\sin(\pi - x)| = |\sin(\pi + x)| = |\sin(2\pi - x)|$ , it is sufficient to consider a uniform distribution for  $0 \leq \phi_s < \pi/2$ , with probability density  $2/\pi$ . In this case,  $\beta$  is a monotonic function of  $\phi_s$ . It is well known that if  $X$  is a random variable of probability density function  $f_X$ , and  $Y = G(X)$  with  $G$  a monotonic function, then the PDF of  $Y$  is  $f_Y(y) = f_X(G^{-1}(y)) \times |(G^{-1})'(y)|$ . Thus, using Eq. (2.1) for fixed  $\Psi$ , the PDF of  $\beta$  is:

$$f(\beta|\Psi) = \begin{cases} \frac{2}{\pi} \frac{1 + \tan^2 \beta}{(\tan^2 \Psi - \tan^2 \beta)^{1/2}} & \text{if } \beta \in \mathcal{T} = \{0 \leq \beta < \Psi < \frac{\pi}{2}\} \cup \{\frac{\pi}{2} < \Psi < \beta \leq \pi\}, \\ 0 & \text{otherwise} \end{cases} \quad (2.2)$$

One can check analytically that  $\int_0^\pi f(\beta|\Psi) d\beta = 1$  for all  $\Psi$ . If now  $\Psi$  has its own PDF  $w(\Psi)$  (such that  $\int_0^\pi w(\Psi) d\Psi = 1$ ), the corresponding PDF of  $\beta$  will be:

$$f(\beta) = \int_{\Psi=0}^{\Psi=\pi} f(\beta|\Psi) w(\Psi) d\Psi. \quad (2.3)$$

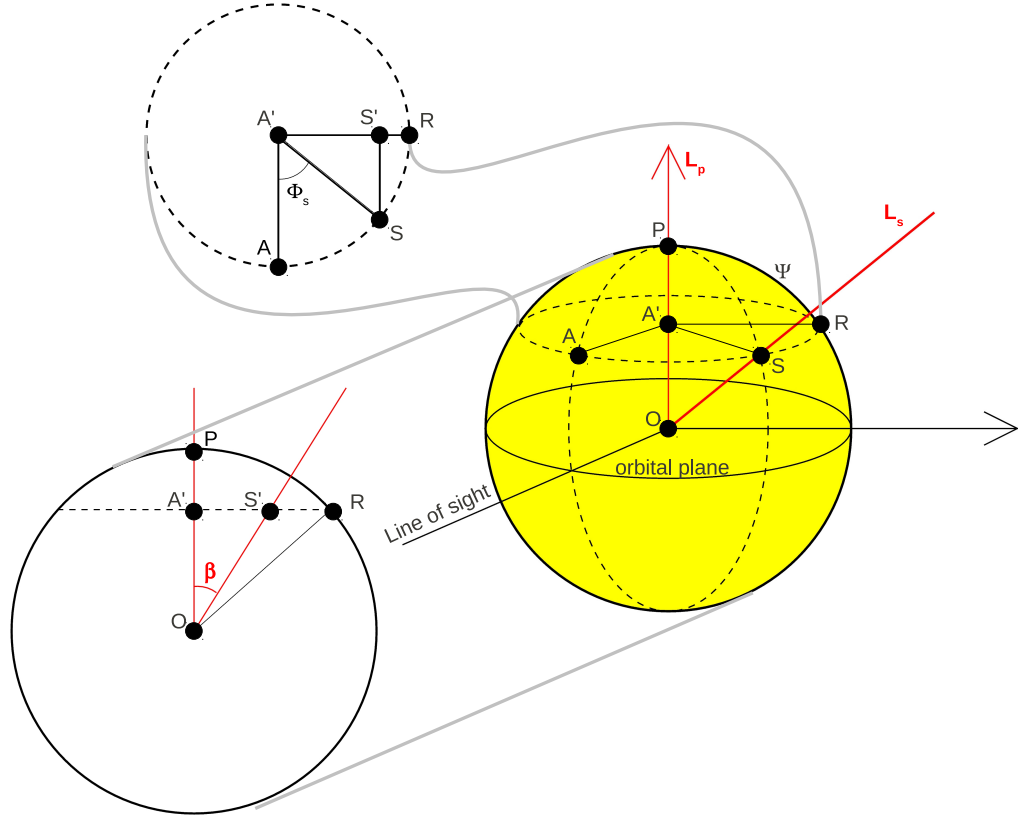


**Fig. 2. Right :** 3D representation of the problem. The yellow sphere is the unit sphere centred on the star. P marks the direction of the orbital angular momentum vector  $\vec{L}_p$  and S that of the stellar spin  $\vec{L}_s$ . The dashed circle passing through points A and S gathers all the points making an angle  $\Psi$  with P. It is represented in the top left.

**Top left :** The circle of the unit sphere gathering all the points at colatitude  $\Psi$  with respect to the orbital angular momentum vector of the planet. A is the point facing the observer ; S is the point corresponding to the direction of the stellar spin. A and S are projected on the diameter of this circle perpendicular to the line of sight onto A' and S' ;  $\phi_s$  is then  $\widehat{AA'S}$ .

**Bottom left :** The projected plane, as seen by the observer. The previous dashed circle is now a dashed horizontal line, on which A' and S' are the projections of A and S along the direction of the line of sight. The arc PR defines an angle  $\Psi$ , while the projected spin orbit angle  $\beta$  is  $\widehat{A'OS'}$ , marked in red.

### 3 Application to proposed mechanisms

#### 3.1 Disk torquing

A simple description of the disk torquing model by Batygin (2012) is the following: the angle between the stellar equatorial plane and the orbital plane of the companion star is  $i'$ , randomly distributed in 3D, that is between 0 and  $\pi/2$  with a PDF  $\sin(i')$ . Then, the disk precesses around this axis, while the star is unperturbed. As a consequence,  $\Psi$  oscillates periodically between 0 and  $2i'$ . When the companion star leaves,  $\Psi$  is fixed, at any value in this interval. This gives to the spin-orbit angle the PDF :

$$w(\Psi) = \frac{1}{2} [\text{Si}(\pi/2) - \text{Si}(\Psi/2)] \quad , \quad \text{where } \text{Si}(x) = \int_0^x \frac{\sin t}{t} dt \quad . \quad (3.1)$$

This function is represented as the thin, almost straight, red line in the left panel of Figure 1. The blue, thick, curved line represents the corresponding PDF of  $\beta$ , as given by Eqs (2.3) and (3.1). The difference between the two curves enlightens the necessity of taking into account the projection effects. The blue curve is in good qualitative agreement with the observed distribution. In fact, the only difference with the observations lies in an underestimation of the proportion of aligned cases. But this shouldn't be a problem: not all stars have a

transient companion during their formation, that perturbs their proto-planetary disk. The excess of aligned cases may simply reflect the fact that in a few systems, the proto-planetary disk have never left the equatorial plane of the star.

To check this, we have performed Monte-Carlo simulations of disk torquing, taking into account the magnetic coupling between the star and the disk (Batygin & Adams 2013), and with random orbital parameters for the binary. We find that the distribution beyond  $\beta > 40^\circ$  is extremely robust. On the other hand, the fraction of aligned systems strongly depends on the distribution of the maximum semi-major axis of the binaries, namely it increases when wider binaries are considered.

### 3.2 Other mechanisms

The left panel of Figure 1 shows the distribution of  $\beta$  that would be given by a few mechanisms found in the literature (see caption). In all three cases, we have taken the PDF of  $\Psi$  provided in the paper, and transformed it into a distribution of  $\beta$  using our Eq. (2.3), in order to compare with the observations (histogram in the background). The distributions have been normalized to have 18 cases with  $\beta > 40^\circ$ , like in the observations.

We see that all of them reproduce satisfactorily the almost flat distribution of  $\beta$  beyond  $60^\circ$ , but all fail at reproducing the observed distribution at  $\beta < 40^\circ$ . In particular, one sees a significant lack of aligned systems. Hence, none of these mechanisms can be responsible for the production of most hot Jupiters.

## 4 Summary

1. The *real* spin-orbit angle  $\Psi$ , is a 3D angle and so lies between 0 and  $180^\circ$ . The *projected* spin-orbit angle  $\beta$  is in the plane of the sky, but its direction (clockwise or counterclockwise) only depends on whether we see the ascending or descending node, and cannot be determined by observations. Reporting negative angles doesn't make sense.
2. We provide an easy way to connect the distributions of the real and projected spin-orbit angles distributions (Eqs (2.2) and (2.3)). Any model pretending to explain the spin-orbit misalignments should be tested against the observed distribution, using this link.
3. About half of the hot Jupiters are well aligned; this can not be explained by the Kozai Cycles with Tidal Friction or scattering models. Thus, at least a third of the hot Jupiters must have been formed by standard type II migration in an aligned disk.
4. Type II migration in a torqued disk also leads to the production of misaligned hot Jupiters, and our analytical model and monte-carlo simulations show that the expected distribution of  $\beta$  in this case is in very good agreement with the observations.

In the end, based solely on the distribution of the observed projected spin-orbit angle, it seems that type II migration could be the dominant mechanism of formation of hot Jupiters, misaligned or not.

## References

- Batygin, K. 2012, *Nature*, 491, 418  
 Batygin, K. & Adams, F. C. 2013, *ApJ*, 778, 169  
 Beaugé, C. & Nesvorný, D. 2012, *ApJ*, 751, 119  
 Crida, A. & Batygin, K. 2014, *A&A*, 567, A42  
 Crida, A. & Morbidelli, A. 2007, *MNRAS*, 377, 1324  
 Fabrycky, D. & Tremaine, S. 2007, *ApJ*, 669, 1298  
 Ford, E. B. & Rasio, F. A. 2008, *ApJ*, 686, 621  
 Lin, D. N. C. & Papaloizou, J. 1986, *ApJ*, 309, 846  
 Mac Laughlin, D. B. 1924, *ApJ*, 60, 22  
 Nagasawa, M., Ida, S., & Bessho, T. 2008, *ApJ*, 678, 498  
 Naoz, S., Farr, W. M., Lithwick, Y., Rasio, F. A., & Teyssandier, J. 2011, *Nature*, 473, 187  
 Rasio, F. A. & Ford, E. B. 1996, *Science*, 274, 954  
 Triaud, A. H. M. J., Collier Cameron, A., Queloz, D., et al. 2010, *A&A*, 524, A25  
 Winn, J. N., Johnson, J. A., Peek, K. M. G., et al. 2007, *ApJ*, 665, L167